Acta Cryst. (1980). A**36**, 22–27

Primary Extinction for Finite Crystals. Cylinder

BY N. M. OLEKHNOVICH AND A. I. OLEKHNOVICH

Institute of Physics of Solids and Semiconductors, Byelorussian Academy of Sciences, Minsk 220726, *USSR*

(*Received* 13 *February* 1978; *accepted* 3 *July* 1979)

Abstract

The results are given for the calculated profile function of the scattering curve and primary extinction factor for a crystal in the form of a cylinder as a function of its diameter τ, expressed in extinction length units and the Bragg angle. The calculations are based on the equations of the dynamical theory of X-ray diffraction. It is shown that the shift of the scattering curve maximum specified by the refraction effect depends on the crystal diameter τ. This shift for normal polarization of the incident X-ray radiation is found to be greater than that for the parallel one but at $\tau \ll 1$ for both polarizations it is the same. Approximate expressions for estimation of the primary extinction factor as a function of τ at different Bragg angles are given.

1. Introduction

The study of X-ray diffraction in finite crystals on the basis of the dynamical theory is of importance in the investigation of X-ray scattering mechanisms in mosaic crystals and in calculating the extinction effects for them. The existing approximations of the theory of X-ray diffraction in mosaic crystals are based on the Darwin–Zachariasen transfer equations (Zachariasen, 1967; Becker & Coppens, 1974) in which, as is known, the dynamic effects of scattering are not taken into account. The investigation of the polarization of X-rays scattered by real crystals (Olekhnovich & Schmidt, 1977) has shown that the transfer equations have a limited range of application. The general theory of extinction for mosaic crystals on the basis of the dynamical diffraction theory equations (Takagi, 1962, 1969; Taupin, 1967) was developed by Kato (1976). However, there are great difficulties in this method.

Using the method of solution of the Takagi–Taupin equations for finite crystals (Uragami, 1969, 1970, 1971; Afanas'ev & Kohn, 1971) we have previously (Olekhnovich & Olekhnovich, 1978) carried out calculations of the primary extinction factor and the angular distribution of diffracted radiation for a crystal block in the form of a square-section parallelepiped. There arises the question of the dependence of the characteristics of scattered radiation on the crystal-block shape. The aim of this paper is to solve the Takagi–Taupin equations for a block in the shape of a circular cylinder, to calculate the primary extinction factor and the profile function of the scattering curve as a function of its diameter.

2. Integral representation for the amplitude and power of radiation diffracted by a cylindrical crystal

According to Afanas'ev & Kohn (1971), the Takagi (1969) equations determining the field amplitudes E_0 and E_1 in a crystal can be written as

$$\frac{\partial^2 \mathscr{E}_{0,1}}{\partial s_0\, \partial s_1} + \sigma^2 \mathscr{E}_{0,1} = 0, \tag{2.1}$$

where

$$\mathscr{E}_{0,1} = E_{0,1} \exp[i\sigma_0(s_0 + s_1) - i\beta_1 s_1], \tag{2.2}$$

$$\sigma_0 = \chi_0 K/2, \quad \sigma = (\sigma_1 \sigma_2)^{1/2}, \quad \sigma_1 = \chi_{-h} CK/2,$$

$$\sigma_2 = \chi_h CK/2,$$

$\beta_1 = \alpha K/2 = \varepsilon K \sin 2\theta_B$ and $\varepsilon = \theta_B - \theta$ is the angular deviation from the Bragg angle. The remaining symbols have their generally accepted meaning.

Let us find expressions for the field amplitudes of the radiation diffracted by the cylindrical crystal, its axis being normal to the scattering plane. The wave incident at s_0 (Fig. 1) on the surface T_0R_0R has amplitude E_0^{in}.

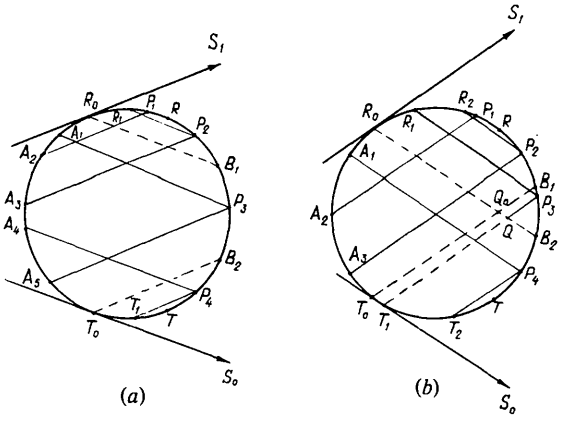

Fig. 1. The scheme of crystal division into the areas for calculation of the diffracted X-ray fields. (*a*) $0 \le \theta_B \le 30°$, (*b*) $30 \le \theta_B \le 45°$.

To determine $\mathscr{E}_1$ we shall use the integral form of the solution for (2.1) as in the case of a square-section parallelepiped:

$$\oint \mathscr{E}_1 \frac{\partial V}{\partial s_0} ds_0 + V \frac{\partial \mathscr{E}_1}{\partial s_1} ds_1 = 0, \qquad (2.3)$$

where V is the Green function.

The Green function depends on the crystal geometry, as it has to fulfil certain boundary conditions at the crystal surface (Uragami, 1969).

For integration contours, including the R_0R area, on which there is only a diffracted wave, the Green function has to fulfil the condition

$$\left.\frac{\partial V_1^R}{\partial s_0}\right|_{R_0R} = 0.$$

Taking into account this condition, we find

$$V_1^R = J_0\{2\sigma[(s_{0P} - s_0)(s_{1P} - s_1)]^{1/2}\} + \frac{\gamma_0^R\{[(s_{1P} - s_{1R_0'})\gamma_1^R/\gamma_0^R] - s_0\}}{\gamma_1^R[(s_{1R_0'} + s_{0p}\gamma_0^R/\gamma_1^R) - s_1]} \times J_2[2\sigma(\{[(s_{1P} - s_{1R_0'})\gamma_1^R/\gamma_0^R] - s_0\} \times [(s_{1R_0'} + s_{0P}\gamma_0^R/\gamma_1^R) - s_1])^{1/2}]. \qquad (2.4)$$

Here J_0 and J_2 are the Bessel functions of zero and second order respectively; $s_{1R_0'} = s_{1R_1} - \gamma_0^R s_{0R_1}/\gamma_1^R$ is the intercept on the axis s_1, which is cut by the trace of the plane R_1R_ψ (Fig. 2), being parallel to the cylinder axis and passing through the points R_1 and R_ψ. R_1 is the point at which the characteristic PR_1 intercepts the cylinder surface contour in the area R_0R. R_ψ is the point of integration coordinate on R_0R. $\gamma_{0,1}^R = |\cos(\mathbf{n}.\mathbf{s}_{0,1})|$. $\mathbf{n}$ is inner normal to the plane R_1R_ψ.

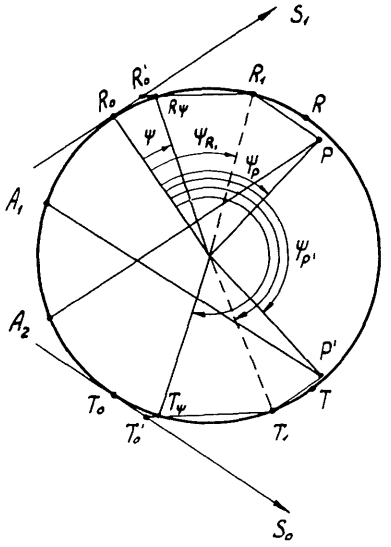

Fig. 2. The scheme of coordinate determination.

If the integration coordinate point is in the range T_0R_0, the point $s_{1R_0'}$ coincides with s_{1R_0}.

On the integration contours, including the area T_0T where $E_1 = 0$, the Green function V_1^T should fulfil the condition $V_1^T|_{T_0T} = 0$. Taking into account this condition V_1^T is determined as follows:

$$V_1^T = J_0\{2\sigma[(s_{0P} - s_0)(s_{1P} - s_1)]^{1/2}\} - J_0[2\sigma([(s_{0T_0'} + s_{1P}\gamma_1^T/\gamma_0^T) - s_0] \times \{[(s_{0P} - s_{0T_0'})\gamma_0^T/\gamma_1^T] - s_1\})^{1/2}]. \qquad (2.5)$$

Here $s_{0T_0'} = s_{0T_1} - \gamma_1^T s_{1T_1}/\gamma_0^T$ is the intercept on the axis s_0 which is cut by the trace of the plane T_1T_ψ (Fig. 2) passing through the points T_1 and T_ψ. T_1 is the interception of the characteristic $P'T_1$ with T_0T. T_ψ is the point of integration coordinate on this area. $\gamma_{0,1}^T = |\cos(\mathbf{n}_T.\mathbf{s}_{0,1})|$, where $\mathbf{n}_T$ is the inner normal to the plane T_1T_ψ. If the integration-coordinate point lies out of the range T_0T then $s_{0T_0'}$ coincides with s_{0T_0}.

In the case of integration contours which do not include R_0R or T_0T, the Green function is determined by one Bessel function of zero order:

$$V_1 = J\{2\sigma[(s_{0P} - s_0)(s_{1P} - s_1)]^{1/2}\}. \qquad (2.6)$$

Expressions (2.4) and (2.5) for the Green function can be used in considering a crystal of any convex form.

As in the case of the square-section parallelepiped, we limit our consideration to the case of the Bragg angle in the range from 0 to 45°. The solution of (2.1) for $\theta_B > 45°$ is more complicated and it will be considered elsewhere.

The case of diffraction when $\theta_B \leq 30°$

The expressions for the amplitude $\mathscr{E}_1$ on the areas R_0R, RB_1, B_1B_2, B_2T of the external crystal surface can be found by applying (2.3) to the contours $A_2P_1R_0A_2$, $A_3P_2R_1R_0A_3$, $A_5P_3A_1A_5$, $T_1P_4A_4T_0T_1$ (Fig. 1*a*), taking into account the corresponding boundary conditions:

$$\mathscr{E}_{1P_1} = -i\sigma_2 \int_{A_2}^{R_0} \mathscr{E}_0^{\text{in}} V_1^R \, ds_1 - i\sigma_2 \int_{R_0}^{P_1} \mathscr{E}_0^{\text{in}} V_1^R \, ds_1, \qquad (2.7)$$

$$\mathscr{E}_{1P_2} = -i\sigma_2 \int_{A_3}^{R_0} \mathscr{E}_0^{\text{in}} V_1^R \, ds_1 - i\sigma_2 \int_{R_0}^{R_1} \mathscr{E}_0^{\text{in}} V_1^R \, ds_1, \qquad (2.8)$$

$$\mathscr{E}_{1P_3} = -i\sigma_2 \int_{A_5}^{A_1} \mathscr{E}_0^{\text{in}} V_1 \, ds_1, \qquad (2.9)$$

$$\mathscr{E}_{1P_4} = -i\sigma_2 \int_{T_0}^{A_4} \mathscr{E}_0^{\text{in}} V_1^T \, ds_1, \qquad (2.10)$$

where $\mathscr{E}_0^{\text{in}}$ is determined by (2.2) using E_0^{in}.

Let us proceed in the polar coordinate system (r, ψ) (Fig. 2). The polar angle ψ being read off clockwise

from the point R_0, the coordinates of the crystal-surface points in the new coordinate system are determined as follows:

$$s_0 = r(1 - \cos\psi)/\sin 2\theta_B,$$
$$s_1 = r[1 + \cos(2\theta_B - \psi)]/\sin 2\theta_B, \quad (2.11)$$

where r is the cylinder radius.

Then the expressions for E_1 in the indicated ranges can be written as

$$E_{1P_1} = \frac{i\sigma_2 r}{\sin 2\theta_B} A_\varphi \left[\int_{-\varphi}^{0} E_0^{\text{in}} A_\psi B \, d\psi + \int_{0}^{\varphi} E_0^{\text{in}} A_\psi D \, d\psi \right], \quad (2.12)$$

$$E_{1P_2} = \frac{i\sigma_2 r}{\sin 2\theta_B} A_\varphi \left[\int_{-\varphi}^{0} E_0^{\text{in}} A_\psi G \, d\psi + \int_{-(4\theta_B-\varphi)}^{0} E_0^{\text{in}} A_\psi L/d\psi + \int_{0}^{4\theta_B-\varphi} E_0^{\text{in}} A_\psi M \, d\psi \right], \quad (2.13)$$

$$E_{1P_3} = \frac{i\sigma_2 r}{\sin 2\theta_B} A_\varphi \int_{-\varphi}^{4\theta_B-\varphi} E_0^{\text{in}} A_\varphi G \, d\psi, \quad (2.14)$$

$$E_{1P_4} = \frac{i\sigma_2 r}{\sin 2\theta_B} A_\varphi \left[\int_{-(\pi-2\theta_B)}^{4\theta_B-\varphi} E_0^{\text{in}} A_\psi G \, d\psi - \int_{-(\pi-2\theta_B)}^{\varphi+4\theta_B-2\pi} E_0^{\text{in}} A_\psi N \, d\psi \right]. \quad (2.15)$$

Here,

$$A_\varphi = \exp[-ik\tau \sin(\theta_B - \varphi)/\cos\theta_B - i\pi\beta\cos(2\theta_B - \varphi)/2], \quad (2.16)$$

$$A_\psi = \exp[ik\tau \sin(\theta_B - \psi)/\cos\theta_B - i\pi\beta\cos(2\theta_B - \psi)/2], \quad (2.17)$$

$$B = [J_0(w_1) + z_1 J_2(w_1)]\sin(2\theta_B - \psi),$$
$$D = [J_0(w_1) + J_2(w_1)]\sin(2\theta_B - \psi),$$
$$G = J_0(w_1)\sin(2\theta_B - \psi),$$
$$L = z_2 J_2(w_2)\sin(2\theta_B - \psi),$$
$$M = [J_0(w_1) + z_3 J_2(w_1)]\sin(2\theta_B - \psi),$$
$$N = J_0(w_3)\sin(2\theta_B - \psi),$$

where

$$w_1 = \frac{\tau}{\sin 2\theta_B}[(\cos\psi - \cos\varphi)[\cos(2\theta_B - \varphi) - \cos(2\theta_B - \psi)]^{1/2},$$

$$w_2 = \frac{\tau}{\sin 2\theta_B}\{2[\cos\psi - \cos(4\theta_B - \varphi)] \times [\sin^3(\varphi/2)/\sin(2\theta_B - \varphi/2) - \sin(\psi/2)\sin(2\theta_B - \psi/2)]\}^{1/2},$$

$$w_3 = \frac{\tau}{\sin 2\theta_B}\{2[\cos(2\theta_B + \varphi) - \cos(\psi - 2\theta_B)] \times [\cos(\psi/2 + \theta_B)\cos(\psi/2 - \theta_B) - \cos^3(\varphi/2 - \theta_B)/\cos(\varphi/2 + \theta_B)]\}^{1/2},$$

$$z_1 = \sin(2\theta_B - \varphi/2)\sin[(\varphi + \psi)/2] \times \{\sin(\varphi/2)\sin[2\theta_B - (\varphi + \psi)/2]\}^{-1},$$

$$z_2 = \sin(\varphi/2)[\cos\psi - \cos(4\theta_B - \varphi)] \times \{2[\sin^3(\varphi/2) - \sin(\psi/2)\sin(2\theta_B - \psi/2) \times \sin(2\theta_B - \varphi/2)]\}^{-1},$$

$$z_3 = [\cos\psi - \cos(4\theta_B - \varphi)]/[\cos\psi - \cos\varphi],$$
$$k = F_0/2C\sqrt{F_h F_{-h}}, \quad (2.18)$$

$\beta = -r\beta_1/\pi\sin 2\theta_B$, $\tau = 2rr_0\lambda C\sqrt{F_h F_{-h}}/v$ is the cylinder diameter, expressed in extinction length units; φ is the polar angle of the point at which the values of the field amplitudes E_1 are found; F_0, F_h and F_{-h} are structure factors for 0, h and $\bar{h}$ reflections respectively; λ is the wavelength of X-ray radiation; v is the unit-cell volume; $r_0 = e^2/mc^2$ is the classical radius of the electron.

The case of diffraction when $30 \le \theta_B \le 45°$

The field amplitude E_1 on the areas R_0R, RB_1 and B_2T at $30 \le \theta_B \le 45°$ will have the same expressions as those given for $\theta_B \le 30°$. To determine the field $\mathscr{E}_1$ in the area B_1B_2 (Fig. 1*b*), (2.3) is applied to the contour $QP_3R_1R_0Q$ and we obtain

$$\mathscr{E}_{1P_3} = \mathscr{E}_{1Q} - i\sigma_2 \int_{R_0}^{R_1} \mathscr{E}_0^{\text{in}} V_1^R \, ds_1 - \int_{R_0}^{Q} \mathscr{E}_1 \frac{\partial V_1^R}{\partial s_0} dS_0. \quad (2.19)$$

Carrying out the necessary transformations in (2.19) and passing to the system of polar coordinates, one gets

$$E_{1P_3} = \frac{i\sigma_2 r}{\sin 2\theta_B} A_\varphi \left[\int_{-(\pi-2\theta_B)}^{0} E_0^{\text{in}} A_\psi G \, d\psi + \int_{-(4\theta_B-\varphi)}^{0} E_0^{\text{in}} A_\psi L \, d\psi + \int_{0}^{4\theta_B-\varphi} E_0^{\text{in}} A_\psi M \, d\psi - \int_{-(\pi-2\theta_B)}^{\varphi+4\theta_B-2\pi} E_0^{\text{in}} A_\psi N \, d\psi \right]. \quad (2.20)$$

The primary extinction factor (y_p) is determined by the following integral:

$$y_p = A^{-1} \int_{-\infty}^{\infty} R(\beta)\, d\beta. \qquad (2.21)$$

Here, $R(\beta)$ is the profile function of the scattering curve for the considered crystal and is determined by the ratio of the diffracted power, at a given angle β, to the integrated diffracted power in the kinematical limit. A is the absorption factor.

If $\theta_B \leq 30°$,

$$R(\beta) = (2\pi \mathscr{P}_0 \sin 2\theta_B)^{-1} \left[\int_0^{2\theta_B} d\varphi I_{1\varphi} \sin\varphi + \int_{2\theta_B}^{4\theta_B} d\varphi I_{2\varphi} \sin\varphi + \int_{4\theta_B}^{\pi-2\theta_B} d\varphi I_{3\varphi} \sin\varphi + \int_{\pi-2\theta_B}^{\pi} d\varphi I_{4\varphi} \sin\varphi \right], \qquad (2.22)$$

where

$$I_{j\varphi} = \left| \frac{\sin 2\theta_B}{i\sigma_2 r} \right|^2 |E_{1P_j}|^2, \quad j = 1, 2, 3, 4. \qquad (2.23)$$

$\mathscr{P}_0$ is the power of the radiation incident on the crystal.

With $30 \leq \theta_B \leq 45°$,

$$R(\beta) = (2\pi \mathscr{P}_0 \sin 2\theta_B)^{-1} \left[\int_0^{2\theta_B} d\varphi I_{1\varphi} \sin\varphi + \int_{2\theta_B}^{\pi-2\theta_B} d\varphi I_{2\varphi} \sin\varphi + \int_{\pi-2\theta_B}^{4\theta_B} d\varphi I_{5\varphi} \sin\varphi + \int_{4\theta_B}^{\pi} d\varphi I_{4\varphi} \sin\varphi \right], \qquad (2.24)$$

where $I_{5\varphi}$ is expressed in terms of the amplitude E_{1P_3}, (2.20), by a relation of the form (2.23).

3. The profile function of the scattering curve and the primary extinction factor

Using the above expressions for E_1, we calculated the function $R(\beta)$ and the primary extinction factor y_p for the cylindrical crystal. The calculations were made for the plane incident wave and non-absorbing crystal using a program written in Fortran.

With no absorption, k (2.18) is a real value determining the X-ray refraction effect for diffraction from a crystal. This effect is revealed in a shift of the scattering curve maximum towards higher angles.

The calculations allowed us to find the dependence of the shift of the maximum of the scattering curve ($\Delta\theta_m$) on the crystal diameter and the Bragg angle (Fig. 3). When analyzing this dependence, the shift of the maximum of the curve $R(\beta)$ was expressed in units of

$$\Delta\theta_m/(\chi_0/\sin 2\theta_B) = \pi\beta_m \cos\theta_B/k\tau.$$

Here β_m is the position of the scattering curve maximum in the scale of β.

The dependence of the shift of the maximum of the scattering curve for the block in the form of a cylinder on the Bragg angle and τ is similar to that for a square-section parallelepiped. As is seen from Fig. 3, in the Laue case ($\theta_B = 0$), the refraction effect is absent. With increasing Bragg angle the shift of the maximum of the scattering curve becomes greater. For a given value of the Bragg angle, the shift of the scattering curve maximum increases with increasing τ. As the cylinder diameter τ, expressed in extinction length units, has different values for the parallel and normal polarizations of the incident radiation ($\tau_\parallel = \tau_\perp \cos 2\theta_B$), the effect of the shift of the maximum of the scattering curve will be greater for normal polarization than for parallel polarization. Fig. 4 gives the profiles of the

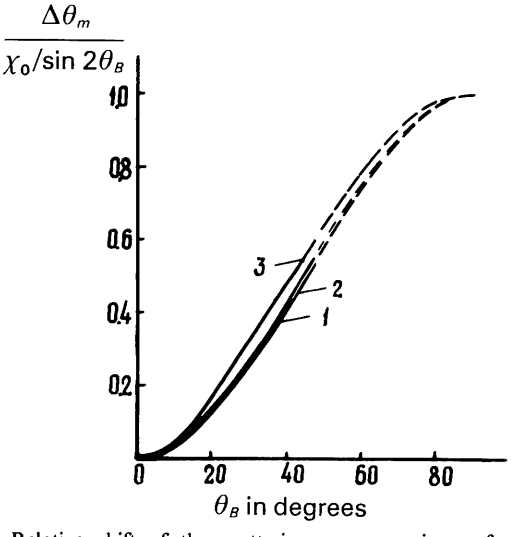

Fig. 3. Relative shift of the scattering curve maximum for the cylinder *vs* the Bragg angle for different values of τ: 1. $\tau = 0{\cdot}1$; 2. $\tau = 1$; 3. $\tau = 2$. Dashed lines – approximate interpolations.

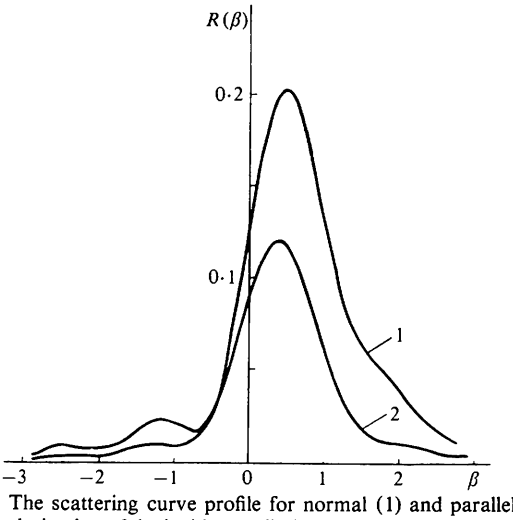

Fig. 4. The scattering curve profile for normal (1) and parallel (2) polarization of the incident radiation at $\tau_\perp = 2$, $\theta_B = 30°$.

calculated scattering curves for the two modes of polarization of the incident radiation in the case where $\tau_\perp = 2$. For the kinematical diffraction case ($\tau \ll 1$), the profiles of the scattering curves for the two modes of polarization coincide.

Fig. 5 shows the profiles of the scattering curves calculated for different values of cylinder diameter. As is seen from this figure, an increase of the crystal diameter leads to the rapid decrease of the $R(\beta)$ value in the principal maximum range, the half-width of the scattering curve increasing. It should be noted that in the kinematic approximation the half-width of the scattering curve in the chosen scale of β might not depend on τ.

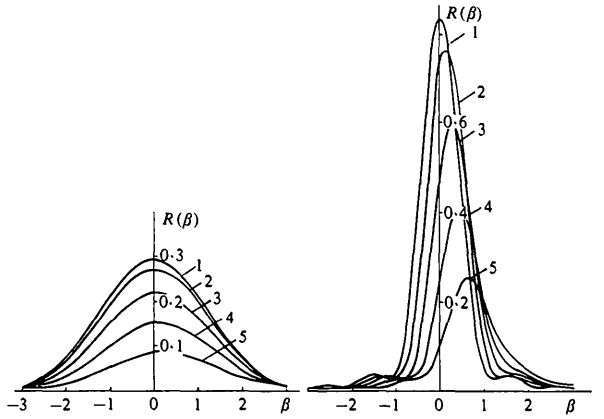

Fig. 5. The profile of the scattering curve for the cylindrical crystal as a function of its diameter: 1. $\tau \ll 1$; 2. $\tau = 0{\cdot}5$; 3. $\tau = 1{\cdot}0$; 4. $\tau = 1{\cdot}5$; 5. $\tau = 2$; with $k = 2$. (*a*) $\theta_B = 10°$, (*b*) $\theta_B = 40°$.

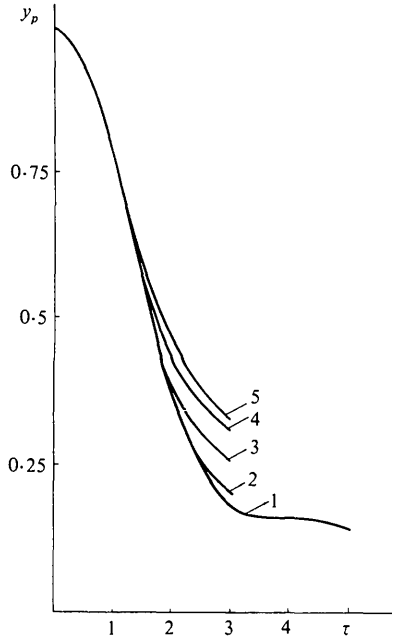

Fig. 6. Primary extinction factor *vs* cylinder diameter for different Bragg angles: 1. 0°; 2. 20°; 3. 30°; 4. 40°; and 5. 45°.

From Fig. 6, it can be seen that the primary extinction factor for the crystal cylinder does not depend on the Bragg angle when its diameter does not exceed the extinction length. When the cylinder diameter exceeds the extinction length, the primary extinction factor is a function of not only τ but also the Bragg angle.

The primary extinction factor can be estimated with an error of 2% using the following approximate expression valid for $3 \geq \tau \geq 0{\cdot}60 + 2{\cdot}32 \cos^4 \theta_B$:

$$y_P = y_P^0\{1 + 0{\cdot}335[\tau - (0{\cdot}60 + 2{\cdot}32 \cos^4 \theta_B)]^{3/2}\} \tag{3.1}$$

and for $\tau < 0{\cdot}60 + 2{\cdot}32 \cos^4 \theta_B$:

$$y_P = y_P^0. \tag{3.2}$$

Here, y_P^0 is the primary extinction factor at $\theta_B = 0$, which, as follows from the solution of (2.1), is determined by the expression:

$$y_P^0 = \frac{2}{\pi}\int_0^\pi d\varphi \sin^2\varphi \int_0^1 J_0^2(\tau\sqrt{1-x^2})\,dx. \tag{3.3}$$

y_P^0 can be estimated with an error of 0·5% with the following approximation, valid for $\tau < 4$:

$$y_P^0 = \exp[-(\tau/2)^2] + 0{\cdot}147 \exp[-0{\cdot}45(\tau - 4{\cdot}2)^2]. \tag{3.4}$$

At $\theta_B = 0$, the primary extinction factor for $\tau > 3$ is weakly affected by oscillation, which is a characteristic of the Laue case.

Conclusions

On the basis of the solution of the equations of the dynamical theory of X-ray diffraction, the primary extinction factor and the profile of the scattering curve for a crystal in the form of a cylinder have been calculated. Earlier, the same calculations were carried out by us (Olekhnovich & Olekhnovich, 1978) for a crystal in the form of a square-section parallelepiped. The comparison of the results of these two calculations makes it possible to determine the dependence of diffraction properties on the crystal shape.

The primary extinction factor for both the cylinder and the square-section parallelepiped, in the case where the crystal size does not exceed the extinction length, does not depend on the Bragg angle and the character of the variation of y_P as a function of τ for both crystal-block shapes is almost the same. For blocks, the size of which exceeds the extinction length ($\tau > 1$), the dependence of y_P on τ is somewhat different, especially at small Bragg angles.

The shift effect of the scattering curve maximum, due to the zero Fourier component of polarizability, in both cases depends on the ratio of the crystal size to the

extinction length. It means that for a given crystal size, the scattering curve in the case of normal polarization of the incident radiation is shifted towards a larger angle than in the case of parallel polarization. The scattering curve shift for both modes of polarization is equal only for $\tau \ll 1$.

We would like to thank the referee for his helpful comments for improvements to the paper.

References

AFANAS'EV, A. M. & KOHN, V. G. (1971). *Acta Cryst.* A**27**, 421–430.

BECKER, P. J. & COPPENS, P. (1974). *Acta Cryst.* A**30**, 129–147.

KATO, N. *Acta Cryst.* (1976). A**32**, 453–466.

OLEKHNOVICH, N. M. & OLEKHNOVICH, A. I. (1978). *Acta Cryst.* A**34**, 321–326.

OLEKHNOVICH, N. M. & SCHMIDT, M. P. (1977). *Izv. Akad. Nauk B. SSR, Fiz.-Mat. Nauk*, **1**, 118–122.

TAKAGI, S. (1962). *Acta Cryst.* **15**, 1311–1312.

TAKAGI, S. (1969). *J. Phys. Soc. Jpn*, **26**, 1239–1253.

TAUPIN, D. (1967). *Acta Cryst.* **23**, 25–28.

URAGAMI, T. (1969). *J. Phys. Soc. Jpn*, **27**, 147–154.

URAGAMI, T. (1970). *J. Phys. Soc. Jpn*, **28**, 1508–1527.

URAGAMI, T. (1971). *J. Phys. Soc. Jpn*, **31**, 1141–1161.

ZACHARIASEN, W. H. (1967). *Acta Cryst.* **23**, 558–564.

Acta Cryst. (1980). A**36**, 27–32

On the Separation of the Unknown Parameters of the Problem of Crystal-Structure Analysis

BY R. ROTHBAUER

Weidenstrasse 11, 6234 *Hattersheim* 3, *Federal Republic of Germany*

(*Received* 26 *April* 1979; *accepted* 3 *July* 1979)

Abstract

The problem of crystal-structure analysis can be given a form which exhibits dual quasi-symmetry. The orthogonality of the Fourier waves and the non-interpenetration of the atoms play a complementary role; this holds not only formally but also with respect to the separation of the coordinates of the atoms and the phases of the structure factors. The remarkable fact that the Patterson function is described by a convolution in direct space, while Sayre's equation is a convolution in reciprocal space may be understood as a part of the symmetry.

Introduction

The kinds of experiments and theoretical procedures which are used for crystal-structure analysis are numerous.

In most cases of structure analysis, the experimental investigations of the crystal to be analysed are restricted to:

the quantitative chemical analysis,

the determination of the density,

the measurement of the Bragg angles of a number of reflexions, sufficient for the calculation of the lattice parameters,

the measurement of the integral intensities of the reflexions with scattering vectors of length less than the reciprocal of the desired resolution of the scattering density function of the crystal.

From the results of these experiments the following properties of the crystal structure, unknown as a whole, can be deduced by routine application of the laws of physics (see textbooks of crystal-structure analysis):

the lattice constants $\mathbf{a}_1$, $\mathbf{a}_2$, $\mathbf{a}_3$ and the volume V of the unit cell,

the number p of the chemical elements contained in the specimen and the numbers $q(\mu)$, $\mu = 1, 2, \ldots, p$, of the atoms of different kinds in its elementary cell,

the moduli $I^{1/2}(\mathbf{m})$ of the structure factors of the scattering density function $\rho(\mathbf{x})$ of the crystal on a relative scale for all lattice points $\mathbf{m}$ with $|\mathbf{m}|^{-1}$ less than the desired resolution,

the form factors $\hat{\rho}_\mu(\mathbf{m})$ and hence the scattering density function $\rho_\mu(\mathbf{x})$, $\mu = 1, 2, \ldots, p$, of the atoms of the structure.

The system of information just described is necessary and sufficient for the application of the routine methods of crystal-structure analysis, now in common use, *e.g. MULTAN* (Germain, Main & Woolfson, 1971). Besides its practical importance, it is also of special theoretical interest because the problem of crystal-structure analysis, based on this class of information, can be formulated in a dual quasi-symmetric way.

0567-7394/80/010027-06$01.00